Far-End Crosstalk Analysis for Stripline with Inhomogeneous Dielectric Layers (IDL)

Yuanzhuo Liu[#1], Shaohui Yong[#2], Yuandong Guo[#3], Jiayi He[#4], Liang Liu[#5], Nick Kutheis[#6], Albert Sutono[*7], Vijay Kunda[*8], Amy Luoh[*9], Yunhui Chu[*10], Xiaoning Ye[*11], DongHyun Kim[#12], Jun Fan[#13]
[#]Electromagnetic Compatibility Laboratory
Missouri University of Science and Technology
Rolla, MO, USA
[1] liuyuanz, [2] sy2m5, [3] ydggdd, [4]hejiay, [5] llmcr, [6]nakk24, [12]dkim, [13]jfan@mst.edu
[*]Datacenter Group
Intel Corporation
Portland, Oregon, USA
[7]albert.sutono, [8]vijay.kunda, [9]yi.amy.h.luoh, [10]yunhui.chu, [11]xiaoning.ye, @intel.com

2021 IEEE International Joint EMC/SI/PI and EMC Europe Symposium | 978-1-6654-4888-8/21/$31.00 ©2021 IEEE | DOI: 10.1109/EMC/SI/PI/EMCEurope52599.2021.9559227

***Abstract*—Far-end crosstalk (FEXT) noise is a critical factor that affects signal integrity performance in high-speed systems. The FEXT level is sensitive to the dielectric inhomogeneity of the stripline in fabricated printed circuit boards (PCB). Stripline is typically modeled as a 2-layer model with core and prepreg layers. However, in reality, the stripline is laminated by multiple inhomogeneous dielectric layers (IDL). The dielectric layers of the stripline are laminated with epoxy resin and glass bundles. The dielectric permittivity (ε_r) of the epoxy resin and glass bundles are different, which causes the inhomogeneity of the dielectric layers while also increasing the FEXT magnitude. Therefore, a typical 2-layer structure is inaccurate to model the FEXT. In this paper, the stripline model is constructed with the core, prepreg, and resin pocket layers. To analyze the stripline with three IDL, a practical superposition method is proposed. A design guideline to mitigate the FEXT level in the stripline design is proposed based on the method.**

***Keywords*—Far-end Crosstalk (FEXT), Stripline, Dielectric Material, Inhomogeneous Dielectric Layers (IDL)**

I. INTRODUCTION

Far-end crosstalk (FEXT) noise is a critical factor that affects the signal integrity performance in high-speed systems with faster data transmission rates and a higher density of circuits [1-3].

In the fabrication procedure of the multilayer printed circuit boards (PCB), the dielectric layers are laminated with epoxy resin and glass bundles, as is shown in Fig. 1. The dielectric permittivity (ε_r) of the epoxy resin and glass bundles are different. The inhomogeneity of the dielectric layers is caused by the different glass fiber weave/content in prepreg and core, prepreg melting during lamination, and epoxy resin property tolerances [4-6].

Stripline is typically modeled as a 2-layer model with core and prepreg layers [7-9]. FEXT between coupled stripline is the superposition of the received even and odd model signals [10]. With this analysis, FEXT is the superposition of the received even and odd model signals. Due to the difference between the dielectric constants (DK) in prepreg and core layers, the phase velocity for even and odd mode signals are not equal, which in return increases the FEXT magnitude [11].

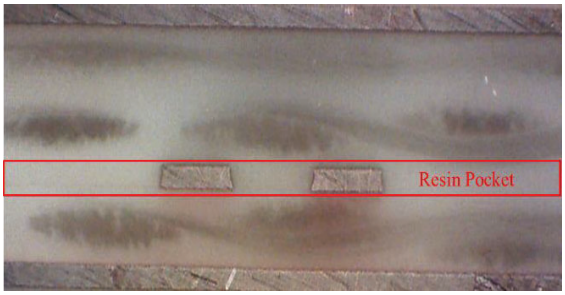

Fig. 1. Cross-section of a pair of coupled stripline. The layer marked with red is the resin pocked.

The normal 2-layer model only takes the inhomogeneity between the core and prepreg layer into account. However, inhomogeneity caused by the epoxy resin and glass bundles inside the core and prepreg layers also affects the FEXT [12]. The 2-layer structure is then not accurate enough to model the stripline performance in the frequency and time domain. The stripline model constructed with multiple inhomogeneous dielectric layers (IDL) with different dielectric permittivity is closer to the performance of the actually fabricated stripline. The resin pocket, which is a layer only filled with resin as shown in Fig. 1, can be considered as a third layer different from the core and prepreg layers. During the lamination of the prepreg layer, some portion of resin melts and forms the resin pocket [13]. Since the resin pocket fills the area between the traces, it plays an important role in stripline modeling. The model of the three IDL can provide a better description of the actual performance of the stripline [14].

In order to analyze, explain and model the processes in multilayer inhomogeneous dielectric layers, a superposition method was proposed. To estimate the FEXT of multiple IDL models, the stripline can be decomposed with 2-layer IDL models. The superposition of each 2-layer IDL model can provide a more accurate FEXT.

Section II introduces the impact of IDL on FEXT by a qualitative theory based on the transmission line theory and analytical expressions. The superposition method for analyzing the stripline model with multiple IDL is proposed and validated in Section III. Section VI analyzes the FEXT of the stripline

with IDL. The proposed superposition method provides a convenient analytical calculation of FEXT caused by the IDL. In addition, a guideline for the stripline with IDL is proposed as a reference for high-speed PCB designers. The proposed method provides an opportunity to better understand the causes of FEXT and develop measures to minimize them.

II. FEXT Analysis Methodology for Stripline with IDL

FEXT is the coupling between transmitting lines as the signal propagates from the transmit end of the pair to the receiving end. To describe the FEXT of coupled striplines, the methodology based on modal analysis is adopted [10]. In a pair of coupled striplines, the aggressor signal is separated into even and odd modes. The odd-mode signal and the even-mode signal propagate through the stripline with different velocities.

The odd and even phase velocities ($v_{p,odd}$, $v_{p,even}$) can be expressed using the per-unit length (PUL) model inductance (L_m) and capacitance (C_m):

$$v_{p,m} = \frac{1}{\sqrt{L_m C_m}} \quad (1)$$

Here, m represents even or odd mode. The FEXT is generated during the time interval between the arrival of the odd-mode signal and the arrival of the even-mode signal.

The differences between $v_{p,even}$ and $v_{p,odd}$ can be described as the variable Δ_{LC}, which is defined as:

$$\Delta_{LC} = L_{odd}C_{odd} - L_{even}C_{even} = 2(L_{11}|C_{21}| - C_{11}L_{21}) \quad (2)$$

To determine the influence of the IDL on Δ_{LC}, the capacitance can be decomposed [15]. In [15, Fig.2], the model with the core and prepreg layer is given. Based on the 2-layer model, the four categories of the per-unit-length capacitances in the 3-layer model shown in Table I are:

TABLE I

Capacitance	Definition
C_f	Fringe capacitance on the outer side of the trace contributed by the prepreg ($C_{f,pg}$) and core ($C_{f,co}$) regions.
C_p	Parallel plate capacitance of the trace, contributed by the prepreg ($C_{p,pg}$) and core ($C_{p,co}$) regions.
C_{fg}	Fringe capacitance near the gap between traces, contributed by the prepreg ($C_{fg,pg}$) and core ($C_{fg,co}$) regions.
C_g	Mutual capacitance across the gap, contributed by the prepreg ($C_{g,pg}$), resin pocket ($C_{g,rp}$) and core ($C_{g,co}$) regions.

Notice that the thickness of the resin pocket is much smaller compared to the thickness of the core and prepreg layer. C_f, C_p, and C_{fg} are dominated by the prepreg and core regions. The mutual capacitance across the gap C_g can be expressed as:

$$\begin{aligned} C_g &= C_{g,pg} + C_{g,co} + C_{g,rp} \\ &= \varepsilon_{r,pg}C^a_{g,pg} + \varepsilon_{r,co}C^a_{g,co} + \varepsilon_{r,rp}\,C^a_{g,rp} \end{aligned} \quad (3)$$

Here, α and β represent the potion of the flux that goes through prepreg and core.

The total capacitance in the prepreg ($C_{t,pg}$) is expressed using the capacitance components with subscript 'pg':

$$\begin{aligned} C_{t,pg} &= C_{f,pg} + C_{p,pg} + C_{fg,pg} \\ &= \varepsilon_{r,pg} \cdot \left(C^a_{f,pg} + C^a_{p,pg} + C^a_{fg,pg}\right) \\ &= \varepsilon_{r,pg} \cdot C^a_{t,pg} \end{aligned} \quad (3.a)$$

This capacitance can be estimated using the scaling of the capacitances in the air-filled line (denoted by the superscript 'a') by the permittivity of the dielectric media [16, Equ. (2.18)]. Similarly, the total capacitance in the core ($C_{t,co}$) is expressed:

$$\begin{aligned} C_{t,co} &= C_{f,co} + C_{p,co} + C_{fg,co} \\ &= \varepsilon_{r,co} \cdot \left(C^a_{f,co} + C^a_{p,co} + C^a_{fg,co}\right) \\ &= \varepsilon_{r,co} \cdot C^a_{t,co} \end{aligned} \quad (3.b)$$

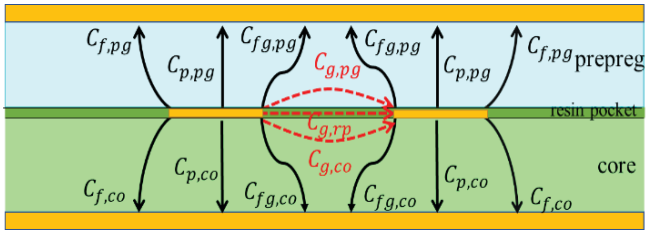

Fig. 2. Illustration of the capacitance components for the coupled striplines. The dielectric permittivity in prepreg, resin pocket, and core are $\varepsilon_{r,pg}$, $\varepsilon_{r,rp}$ and $\varepsilon_{r,co}$ respectively.

Thus, the self-capacitance in the nodal capacitance matrix can be expressed as:

$$\begin{aligned} C_{11} &= C_{t,pg} + C_{t,co} + C_g \\ &= \varepsilon_{r,pg} \cdot C^a_{t,pg} + \varepsilon_{r,co} \cdot C^a_{t,co} \\ &\quad + \varepsilon_{r,pg}C^a_{g,pg} + \varepsilon_{r,co}C^a_{g,co} + \varepsilon_{r,rp}\,C^a_{g,rp} \end{aligned} \quad (4)$$

The mutual-capacitance in the nodal capacitance matrix:

$$|C_{21}| = C_g = \varepsilon_{r,pg}C^a_{g,pg} + \varepsilon_{r,co}C^a_{g,co} + \varepsilon_{r,rp}\,C^a_{g,rp} \quad (5)$$

According to [12, Equ.14] [13, Equ. 14], the self-inductance and mutual-inductance can be estimated using capacitances of the air-filled line as:

$$L_{11}\left[\frac{\text{nH}}{\text{cm}}\right] \approx \frac{10C^a_{11}}{9\Delta C^a}$$

$$= \frac{10\left(C^a_{t,pg} + C^a_{t,co} + C^a_g\right)[\mathrm{pF/cm}]}{9\Delta C^a\ [(\mathrm{pF/cm})^2]} \quad (6)$$

$$L_{21}\left[\frac{\mathrm{nH}}{\mathrm{cm}}\right] \approx \frac{10|C^a_{21}|}{9\Delta C^a} = \frac{10\left(C^a_{g,pg} + C^a_{g,co} + C^a_{g,rp}\right)[\mathrm{pF/cm}]}{9\Delta C^a[(\mathrm{pF/cm})^2]} \quad (7)$$

Where $\Delta C^a = (C^a_{11})^2 - (C^a_{21})^2$. For typical edge-coupled striplines $\Delta C^a > 0$. Then, Δ_{LC} is defined by (2) using the L and C given by (4)-(7) expressed as:

$$\Delta_{LC} = \frac{10}{9\Delta C^a} \cdot [\left(\varepsilon_{r,pg} - \varepsilon_{r,rp}\right) \cdot \left(C^a_{t,pg}C^a_{g,co} - C^a_{t,co}C^a_{g,pg} + C^a_{t,pg}C^a_{g,rp}\right) + \left(\varepsilon_{r,co} - \varepsilon_{r,rp}\right) \cdot \left(C^a_{t,co}C^a_{g,pg} - C^a_{t,pg}C^a_{g,co} + C^a_{t,co}C^a_{g,rp}\right)] \quad (8)$$

$C^a_{t,pg}$, $C^a_{t,co}$, $C^a_{g,pg}$, $C^a_{g,co}$, $C^a_{g,rp}$, ΔC^a are determined by the structure. From (8), it can be noted that Δ_{LC} is proportional to the dielectric permittivity difference between prepreg and resin pocket $\left(\varepsilon_{r,pg} - \varepsilon_{r,rp}\right)$ and the difference between the core and resin pocket $\left(\varepsilon_{r,co} - \varepsilon_{r,rp}\right)$. In other words, the FEXT caused by the 3-layer IDL can be separated into two parts: FEXT caused by the inhomogeneity of prepreg and resin pocket layers and FEXT caused by the inhomogeneity of core and resin pocket layers. Accordingly, the superposition method is introduced in Section III.

III. Superposition Method

To simplify the analysis of the stripline with IDL, the 3-layer model can be decomposed as two 2-layer models. As shown in Fig. 3. Case 1 is the original 3-layer model. The dielectric permittivity in the prepreg, resin pocket, and core layers are $\varepsilon_{r,pg}$, $\varepsilon_{r,rp}$ and $\varepsilon_{r,co}$ respectively. Two inhomogeneous boundaries exist in this model: the boundary between prepreg and resin pocket and the boundary between resin pocket and core. The basic idea is to decompose the two boundaries into two models individually.

In Case 2, the dielectric permittivity of the prepreg layer is set to be $\varepsilon_{r,rp}$, which is the same as the dielectric permittivity of the resin pocket. The model in Case 2 then becomes a 2-layer model with only one inhomogeneous boundary between the resin pocket and core. According to (8), Δ_{LC} of Case 2 is:

$$\Delta_{LC2} = \frac{10C^a_g}{9\Delta C^a} \cdot [\left(\varepsilon_{r,pg} - \varepsilon_{r,rp}\right) \cdot \left(C^a_{t,pg}C^a_{g,co} - C^a_{t,co}C^a_{g,pg} + C^a_{t,pg}C^a_{g,rp}\right)] \quad (9)$$

In Case 3, the dielectric permittivity of the core layer is set to be $\varepsilon_{r,rp}$, which is the same as the dielectric permittivity of the resin pocket. The model in Case 3 then becomes a 2-layer model with only one inhomogeneous boundary between the resin pocket and prepreg.

$$\Delta_{LC3} = \frac{10C^a_g}{9\Delta C^a} \cdot [\left(\varepsilon_{r,co} - \varepsilon_{r,rp}\right) \cdot \left(C^a_{t,co}C^a_{g,pg} - C^a_{t,pg}C^a_{g,co} + C^a_{t,co}C^a_{g,rp}\right)] \quad (10)$$

It can be assumed that the air-filled mutual capacitances across the gap contributed by each layer ($C^a_{g,pg}$, $C^a_{g,co}$, $C^a_{g,rp}$) remain the same when assigning different dielectric permittivity to the layers. Δ_{LC1} can be expressed by the superposition of Case 2 and Case 3:

$$\Delta_{LC1} = \Delta_{LC2} + \Delta_{LC3} \quad (11)$$

Then the FEXT caused by the inhomogeneity of the stripline with the 3 IDL model is equivalent to the superposition of the FEXT of two 2-layer models.

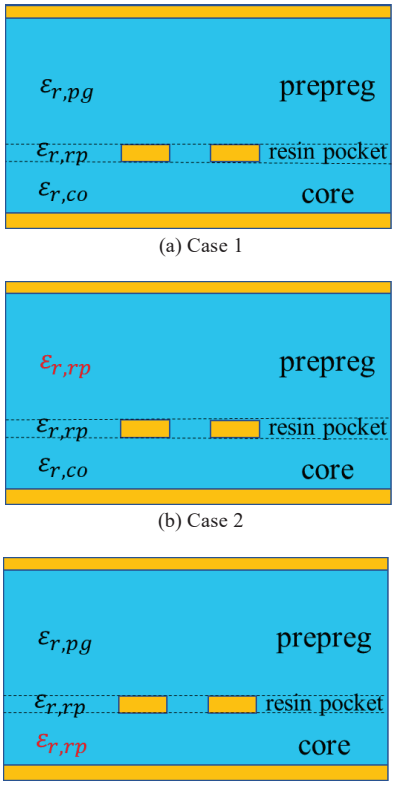

Fig. 3. (a) Case 1: The dielectric permittivity in the prepreg, resin pocket, and core layers are $\varepsilon_{r,pg}$, $\varepsilon_{r,rp}$ and $\varepsilon_{r,co}$ respectively. (b) Case 2: The dielectric permittivity in prepreg and resin pocket layers is $\varepsilon_{r,rp}$. (c) Case 3: The dielectric permittivity in core and resin pocket layers is $\varepsilon_{r,rp}$.

IV. FEXT Analysis for Stripline with IDL

In this section, two examples are given of the FEXT analysis for the stripline with IDL and with different geometries.

A. Example with symmetric geometry

The stripline is normally considered as the combination of two layers: core and prepreg. In this way, only the inhomogeneous between the core and prepreg layer is taken into account for the FEXT analysis. However, inhomogeneous caused by the resin pocket will also affect the FEXT level.

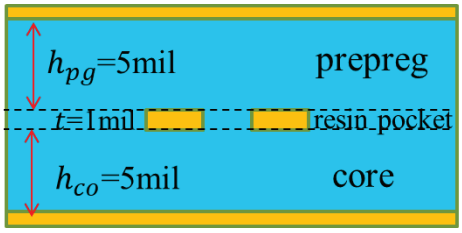

Fig.4. Cross-section geometry of two coupled symmetrical stripline traces. The trace width of the trace is 7.2mil. The spacing between the traces is 10mil.

For example, Fig. 4 demonstrates a cross-section of the stripline. Both the thickness of the prepreg layer and the core layer is 5mil. Both the dielectric permittivity in core and prepreg is 4. The dielectric permittivity in the resin pocket is 2.8. The thickness of the trace, which is also the thickness of the resin pocket layer. The FEXT level of the example can be decomposed with two cases as Fig. 3. All three cases are simulated by ANSYS Q2D. The assignment of dielectric permittivity for the different cases are:

Case 1: $\varepsilon_{r,pg}$=4; $\varepsilon_{r,rp}$=2.8, $\varepsilon_{r,co}$=4.

Case 3: $\varepsilon_{r,pg}$=2.8; $\varepsilon_{r,rp}$=2.8, $\varepsilon_{r,co}$=4.

Case 2: $\varepsilon_{r,pg}$=4; $\varepsilon_{r,rp}$=2.8, $\varepsilon_{r,co}$=2.8.

The transformed FEXT waveform result from the S-parameter of the Q2D simulation is shown in Fig.5. Table II lists the peak value of the FEXT waveform of the three cases. The FEXT level of Case 1 is approximately equal to the sum of Case 2 and Case 3. The error is caused by the assumption during the derivation that the air-filled mutual capacitances across the gap contributed by each layer ($C^a_{g,pg}$, $C^a_{g,co}$, $C^a_{g,rp}$) are the same in different cases. The flux lines tend to get more concentrated in the region with higher dielectric permittivity. As a result, for different cases, the potion of the mutual capacitance contributed by different layers will be slightly different.

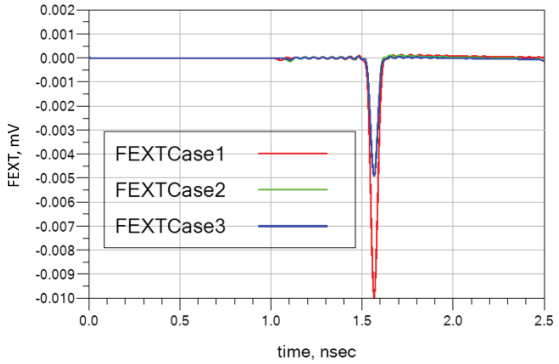

Fig.5. FEXT waveform for the stripline model with the geometry in Fig.4.

TABLE II
The peak value of the FEXT waveform with the geometry in Fig.4

	Case 1	Case 2	Case 3
ε_{preg}	4	2.8	4
ε_{resin}	2.8	2.8	2.8
ε_{core}	4	4	2.8
FEXT Peak (mV)	-9.97	-4.96	-4.96

In this example, the core layer and the prepreg layer have the same thickness and dielectric. If the stripline is only modeled with core and prepreg layers, the mutual capacitance across the gap C_g can be expressed as:

$$C_g = C_{g,pg} + C_{g,co} = \varepsilon_{r,pg}{}' C^a_{g,pg}{}' + \varepsilon_{r,co}{}' C^a_{g,co}{}' \quad (9)$$

Then replace (3) by (9) for (4-7), the Δ_{LC} for the 2-layer model is:

$$\Delta'_{LC} = \frac{10}{9\Delta C^a} \cdot \left(\varepsilon_{r,pg}{}' - \varepsilon_{r,co}{}'\right) \cdot \left(C^a_{t,pg} C^a_{g,co}{}' - C^a_{t,co} C^a_{g,pg}{}'\right) \quad (10)$$

$\varepsilon_{r,pg}{}'$ are $\varepsilon_{r,co}{}'$ are effective dielectric permittivity for the prepreg and core layers in the 2-layer model. $C^a_{g,pg}{}'$, $C^a_{g,co}{}'$ are effective air-filled mutual capacitances across the gap contributed by prepreg and core layers. Thus, the FEXT level by this equivalent model is close to zero. Therefore, in this extreme symmetric example, the normal 2-layer model of the stripline can't perform accurately with multiple IDL.

B. Example with asymmetric geometry

An example with asymmetrical geometry, which is more common in actual PCB design, is simulated and analyzed. The cross-section geometry is shown in Fig. 6. The thickness of the prepreg layer is 7mil, while the thickness of the core layer is 3mil. The dielectric permittivity in the core is 3.5. The dielectric permittivity in the resin pocket is 2.8. In fabricated multi-layer PCB, due to the different glass fiber weave/content in prepreg and core, prepreg melting during lamination, and epoxy resin properties tolerances, etc. [4-6], the dielectric permittivity in the prepreg and core layer are different in this example. Where the dielectric permittivity prepreg is set to be 3.5, 4.5, and 5.5 for different series of the cases.

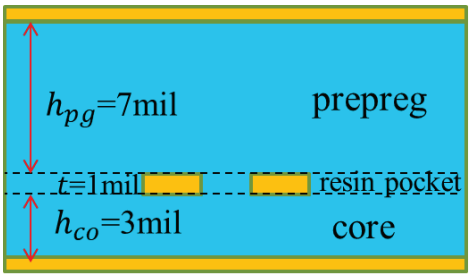

Fig.6. Cross-section geometry of two coupled stripline traces. The trace width of the trace is 7.2mil. The spacing between the traces is 10mil.

Table III lists the FEXT level of the cases. For the series of Case a, Case b, and Case c, the FEXT level of Case x.1 is approximately equal to the sum of Case x.2 and Case x.3 (x can be a, b or c), which provides the verification for the superposition method.

For this example, with asymmetrical geometry, it is difficult to analyze the FEXT directly from the 3-layer model. The superposition method can help by decomposing the total FEXT to two 2-layer cases. In (9) and (10), it can be noted that Δ_{LC} is not only related to the difference of the dielectric material, but

also the capacitance. Then, (9) and (10) can be modified as:

$$\Delta_{LC2}=\frac{10C_g^a}{9\Delta C^a}\cdot\{(\varepsilon_{r,pg}-\varepsilon_{r,rp})\cdot([C_{t,pg}^a\cdot(C_{g,co}^a+C_{g,rp}^a)-C_{t,co}^aC_{g,pg}^a])\} \quad (11)$$

$$\Delta_{LC3}=\frac{10C_g^a}{9\Delta C^a}\cdot\{(\varepsilon_{r,co}-\varepsilon_{r,rp})\cdot[C_{t,co}^a\cdot(C_{g,pg}^a+C_{g,rp}^a)-C_{t,pg}^aC_{g,co}^a]\} \quad (12)$$

In this example, the thickness of the prepreg layer is larger than that of the core layer. As the result, $C_{t,pg}^a$ will be smaller than $C_{t,co}^a$. Considering that the $C_{g,pg}^a+C_{g,rp}^a$ should be larger than $C_{g,co}^a$, Δ_{LC3} is expected to be a positive value. The value of the capacitance term in Δ_{LC2} is expected to be much smaller than that in Δ_{LC3}.

TABLE III Peak value of the FEXT waveform with the geometry in Fig.6

(a)

	Case a.1	**Case a.2**	**Case a.3**
ε_{preg}	3.5	2.8	3.5
ε_{resin}	2.8	2.8	2.8
ε_{core}	3.5	3.5	2.8
FEXT Peak (mV)	-3.65	-6.50	2.95

(b)

	Case b.1	**Case b.2**	**Case b.3**
ε_{preg}	4.5	2.8	4.5
ε_{resin}	2.8	2.8	2.8
ε_{core}	3.5	3.5	2.8
FEXT Peak (mV)	0.30	-6.50	6.69

(c)

	Case c.1	**Case c.2**	**Case c.3**
ε_{preg}	5.5	2.8	5.5
ε_{resin}	2.8	2.8	2.8
ε_{core}	3.5	3.5	2.8
FEXT Peak (mV)	3.91	-6.50	10.63

In practice, to improve the signal integrity performance in high-speed systems, the FEXT is always expected to be mitigated in the design procedure. In the design procedure of the stripline, the method to mitigate the FEXT level could help provide the value $\varepsilon_{r,pg}$ and $\varepsilon_{r,co}$ as a guideline. From (11) and (12), both Δ_{LC2} and Δ_{LC3} are proportional to the difference of the dielectric permittivity while the capacitance term is mainly determined by the cross-section geometry. Therefore, the FEXT caused from Case 2 and Case 3 can be expressed approximately as:

$$FEXT_2 \sim K_2\cdot(\varepsilon_{r,pg}-\varepsilon_{r,rp}) \quad (13)$$

$$FEXT_3 \sim K_3\cdot(\varepsilon_{r,co}-\varepsilon_{r,rp}) \quad (14)$$

K_2 and K_3 can be obtained by two simulations of 2-layer models. For example, from Case a.2 and Case a.3, K_2 is calculated as 4.2 and K_3 is calculated as -9.3. Then the prediction for the total FEXT caused by IDL is:

$$FEXT_{predict}=K_2\cdot(\varepsilon_{r,pg}-\varepsilon_{r,rp})+K_3\cdot(\varepsilon_{r,co}-\varepsilon_{r,rp}) \quad (15)$$

When the $\varepsilon_{r,rp}$ and $\varepsilon_{r,co}$ is known as 2.8 and 3.5, to minimize the FEXT, the $\varepsilon_{r,pg}$ can be determined as 4.35. From Table II(b), when $\varepsilon_{r,pg}$ is 4.5, the total FEXT is 0.3mV. The error between the solution of the prediction and the actual value is 3%. With the superposition method, only two simulations of 2-layer models are needed to predict the FEXT level with different dielectric materials that provide a solution to minimize the FEXT.

V. Conclusion

This paper proposes a practical method to analyze the FEXT for the stripline with IDL and provides a design guideline to mitigate the FEXT level. The 3-layer stripline model constructed with core, prepreg, and resin pocket layers are investigated. The resin pocket is a critical layer with stable dielectric permittivity that locates surrounding traces. The FEXT for the stripline with multilayer IDL can be decomposed with the models that only with one inhomogeneity boundary.

For the stripline with fixed geometry, the FEXT level of the material with different dielectric constant can be expressed. Besides, the best solution of the dielectric constant assignment in the stripline with minimum FEXT can be calculated. This method can be further applied for the construction of stripe lines with multiple IDL and for FEXT analysis of microstrip constructed with layers of a dielectric substrate and a solder mask

Acknowledgment

This work was supported in part by the National Science Foundation (NSF) under Grant IIP-1916535.

References

[1] B. Chen, M. Ouyang, S. Yong, Y. Wang, Y. Bai, Y. Zhou, J. Fan, "Differential integrated crosstalk noise (ICN) reduction among multiple differential BGA and Via pairs by using design of experiments (DoE) method," in *Proc. IEEE Int. Symp. EMC*, Washington, DC, 2017, pp. 112-117

[2] B. Chen, S. Pan, J. Wang, S. Yong, M. Ouyang and J. Fan, "Differential Crosstalk Mitigation in the Pin Field Area of SerDes Channel With Trace Routing Guidance," *IEEE Trans. Electromagn Compat*, vol. 61, no. 4, pp. 1385-1394, Aug. 2019.

[3] B. Chen et al., "Differential Integrated Crosstalk Noise (ICN) Mitigation in the Pin Field Area of SerDes Channel," *Proc. IEEE Int. Symp. EMC*, Long Beach, CA, 2018, pp. 533-537

[4] G. Brist, 'Design Optimization of Single-Ended and Differential Impedance PCB Transmission Lines', Intel Corp., accessed April, 2019. https://www.jlab.org/eng/eecad/pdf/053designop.pdf

[5] X. Tian, Y. Zhang, J. Lim, K. Qiu, R. Brooks, J. Zhang, J. Fan, "Numerical investigation of glass-weave effects on high-speed interconnects in printed circuit board", in *Proc. IEEE Int. Symp. EMC*, Raleigh, NC, USA, Aug. 4–8, 2014, pp. 475–479.

[6] D. Nozadze, A. Koul, K. Nalla, M. Sapozhnikov, V. Khilkevich, 'Effect of time delay skew on differential insertion loss in weak and strong coupled PCB traces', in *Proc. of IEEE Conference on EPEPS*, Oct. 15-18, 2017, San Jose, CA

[7] S. Yong, et al., 'Prepreg And Core Dielectric Permittivity (ε_r) Extraction for Fabricated Striplines', *IEEE Trans. on Electromag. Compat*, under review.

[8] S. Yong, Y. Liu, et al., "Dielectric Dissipation Factor (DF) Extraction Based on Differential Measurements and 2-D Cross-sectional Analysis," 2018 IEEE Symposium on Electromagnetic Compatibility, Signal Integrity and Power Integrity (EMC, SI & PI), Long Beach, CA, 2018, pp. 217-222.

[9] S. Yong et al., "Dielectric Loss Tangent Extraction Using Modal Measurements and 2-D Cross-Sectional Analysis for Multilayer PCBs," in IEEE Transactions on Electromagnetic Compatibility, vol. 62, no. 4, pp. 1278-1292, Aug. 2020, doi: 10.1109/TEMC.2019.2949021.

[10] S. H. Hall, H. L. Heck, *Advanced Signal Integrity for High-Speed Digital Designs*. A John Wiley &. Sons, INC., 2009

[11] S. Yong, V. Khilkevich, X-D. Cai, C. Sui, B. Sen, J. Fan, 'Comprehensive and Practical Way to Look at Far-End Crosstalk for Transmission Lines with Lossy Conductor and Dielectric', *IEEE Trans. on Electromag. Compat*, 2019

[12] B. Zhao, Z. Chen and D. Becker, "Impacts of Anisotropic Permittivity on PCB Trace and Via Modeling," *2018 IEEE 27th Conference on Electrical Performance of Electronic Packaging and Systems (EPEPS)*, San Jose, CA, 2018, pp. 39-41, doi: 10.1109/EPEPS.2018.8534295.

[13] R. Marani, D. Palumbo, U. Galietti, E. Stella and T. D'Orazio, "Two-dimensional cross-correlation for defect detection in composite materials inspected by lock-in thermography," 2017 22nd International Conference on Digital Signa1 Processing (DSP), London, 2017, pp. 1-5, doi: 10.1109/ICDSP.2017.8096090.

[14] Y. Guo, B. Chen, X. Sun, X. Ye, J. Hsu and J. Fan, "Study of TDR Impedance for Better Analysis to Measurement Correlation," *2019 Joint International Symposium on Electromagnetic Compatibility, Sapporo and Asia-Pacific International Symposium on Electromagnetic Compatibility (EMC Sapporo/APEMC),* Sapporo, Japan, 2019, pp. 88-91, doi: 10.23919/EMCTokyo.2019.8893833.

[15] S. S. Bedair, 'Characteristics of Some Asymmetrical Coupled Transmission Lines', IEEE Transactions on Microwave Theory and Techniques, Vol.32, No.1, 1984

[16] S. S. Bedair and I. Wolff, "Fast and accurate analytic formulas for calculating the parameters of a general broadside-coupled coplanar waveguide for (M)MIC applications," in *IEEE Transactions on Microwave Theory and Techniques*, vol. 37, no. 5, pp. 843-850, May 1989, doi: 10.1109/22.17450.